Available online at www.eccomasproceedia.org
Eccomas Proceedia COMPDYN (2025) 41 - 42

ECCOMAS
Proceedia

COMPDYN 2025
10th ECCOMAS Thematic Conference on
Computational Methods in Structural Dynamics and Earthquake Engineering
M. Papadrakakis, M. Fragiadakis (eds.)
Rhodes Island, Greece, 15-18 June 2025

# GENETIC ALGORITHM-BASED OPTIMIZATION OF BOLTED T-STUB CONNECTION UNDER DYNAMIC LOADING USING FINITE ELEMENT ANALYSIS

**Péter Grubits**[1], **Ákos Wolf**[1], **and Majid M. Rad**[1]

[1] Department of Structural and Geotechnical Engineering, Széchenyi István University
Győr, Hungary
e-mail: grubits.peter@sze.hu, wolf@sze.hu, majidmr@sze.hu

**Abstract**

*The equivalent T-stub technique is widely utilized as a design solution for steel bolted connections, which are otherwise complex to analyze. However, traditional standard-based methods often lack the precision required for accurate analysis, particularly when accounting for dynamic effects, such as those caused by earthquakes, leading to designs that may not be sustainable. This research addresses this issue by introducing a framework aimed at optimizing the bolt layout in a selected T-stub connection to maximize structural performance under cyclic loading, thereby enhancing sustainability. The finite element method (FEM) was employed to account for nonlinear characteristics, including the elastic-plastic behavior of steel, large deformations, and contact nonlinearities, ensuring precise analysis. The developed T-stub model was validated against experimental tests to reflect real-world behavior, utilizing ABAQUS finite element software. Optimization was conducted using a genetic algorithm (GA) implemented in the PYTHON programming language, linked to the simulation process. The results demonstrate the effectiveness of the proposed framework in significantly enhancing the structural performance of the steel T-stub connection under cyclic loading conditions without requiring additional material, thereby contributing to a more sustainable design.*

**Keywords:** Finite Element Modelling, Equivalent T-stub, Genetic Algorithm, Optimization, Dynamic Loading.

ISSN:2623-3347 © 2025 The Authors. Published by Eccomas Proceedia.
Peer-review under responsibility of the organizing committee of COMPDYN 2025.
doi: 10.7712/120125.12662.25059

## 1 INTRODUCTION

Bolted connections are commonly employed in steel constructions due to their dual advantage of enabling modular assembly [1] while providing high load-bearing capacity [2]. Consequently, these solutions are widely used across various subfields, including frames [3,4], towers [5,6], and bridges [7]. To address the complexities associated with these joints, the equivalent T-stub method, as defined in Eurocode [8], can be applied. This approach involves discretizing the connection into a series of T-stub components, as illustrated in Figure 1.

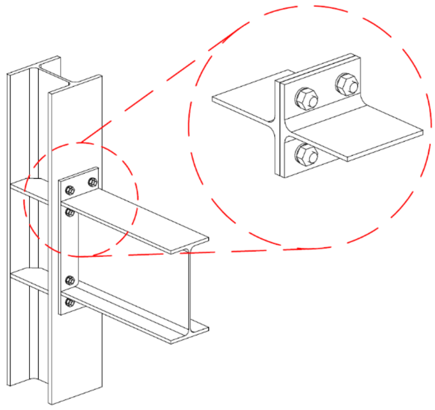

Figure 1: The equivalent T-stub component in the case of a steel beam-column joint.

However, connection design must be carefully considered to prevent progressive collapse under accidental loading, including earthquakes, as joints play a crucial role in governing the structure's ductility and deformation capacity [9,10]. Therefore, advanced approaches, like the finite element method (FEM), should be employed to accurately predict the structural behavior of connections while incorporating nonlinear effects, such as elasto-plastic material properties and large deformations. This enables a more precise analysis compared to traditional code-based methods [11], resulting in a cost-efficient and safe design, which in turn contributes to increased sustainability.

In the last few decades, FEM has proven its potential and effectiveness across various engineering applications [12–14], including the precise simulation of T-stub components under different conditions. Among the early applications, the pioneering work of Bursi and Jaspart [15] stands out, as a benchmark for FEM validation in modeling T-stub elements was established in the proposed study. Later, Al-Khatab and Bouchaïr investigated the effects of strengthening backing plates, incorporating nonlinear material properties, contact interactions, and large deformations [16], while Bravo and Hererra analyzed the performance of T-moment connections under cyclic loading [17]. Furthermore, recent studies have increasingly focused on various loading conditions, as presented in [18–21].

As indicated by these research works, FEM enables accurate structural analysis. However, balancing safety and cost-efficiency to achieve a sustainable design remains a complex and discrete task, particularly under accidental loading conditions such as earthquakes [22,23]. During seismic events, enhancing structural resilience is crucial and can be achieved by minimizing seismic damage [24].

To address these challenges, this paper presents an optimization framework for the design of bolted T-stub connections under dynamic loading, integrating nonlinear finite element analysis (FEA) with a genetic algorithm (GA). The proposed methodology was tested on a validated T-stub model, constructed using ABAQUS software [25], to ensure the reliability of the outcomes. The primary objective of applying the developed approach was to minimize plastic deformations by optimizing the bolt layout. The results indicate that optimal bolt positioning can significantly reduce plastic strains during cyclic loading, thereby mitigating damage under accidental loads without requiring additional material, ultimately contributing to a more sustainable design. This aspect highlights the potential and effectiveness of the developed framework.

## 2 BASIS OF THEORY

This section provides a brief overview of the theoretical foundation underlying this research, which was utilized to develop the proposed framework. It covers the fundamental principles of the genetic algorithm and the key components of elastic-plastic material behavior.

### 2.1 The basic principles of genetic algorithm

Among the various types of heuristic optimization methods, the genetic algorithm (GA) [26] is one of the most frequently used due to its versatility across a wide range of practical applications [27]. In addition, GA is particularly effective for solving nonlinear optimization problems, as its solution technique helps prevent convergence to local minima, even in cases of large search spaces, and does not rely on an assumed initial model. As a result, this approach is well-suited for addressing a variety of structural optimization tasks [28–30].

The fundamental concept of a GA is to mimic natural evolution through a specified number of generations to minimize or maximize the objective function. Throughout the process, the fitness value serves as a metric for assessing the quality of individual solutions within the population [31], referred to as chromosomes. These chromosomes encode the key characteristics of the configuration, which are adjusted during the optimization and selected from the design space. In GA, evolutionary operators are employed to generate the offspring population based on fitness values, including selection, crossover, and mutation.

Selection is responsible for creating the mating pool, which consists of potential parents for the next generation [32]. Among various selection mechanisms, tournament selection is one of the most commonly used. This method involves organizing a tournament among $N$ competitors, where the winner is determined based on the highest or lowest fitness value and is subsequently included in the mating pool [33]. The next step in the process is crossover, where selected solutions are combined to generate offspring. One commonly used approach is the uniform crossover technique, in which either the offspring inherit identical traits from their parents or randomly selected chromosomes are combined. This process is governed by the crossover probability. Finally, mutation is performed, introducing random alterations to the chromosomes based on the mutation probability, thereby maintaining genetic diversity within the population.

### 2.2 Elastic-plastic material

During high-intensity loading, including internal forces induced by earthquakes, steel structures can undergo inelastic deformations that persist after unloading. Consequently, ensuring a safe design requires the assessment and control of these deformations. Therefore, in this study, the plastic strains were employed to assess structural performance.

The actual strain $\varepsilon$ of an elasto-plastic element can be divided into elastic and plastic parts:

$$\varepsilon = \varepsilon^{el} + \varepsilon^{pl} \tag{1}$$

where $\varepsilon^{el}$ denotes the elastic strain corresponding to $\sigma^{el}$ stresses, which represent the response of the material if it were purely elastic. The relationship between these two quantities can be expressed using the elasticity matrix $C^{el}$ as follows:

$$\varepsilon^{el} = C^{el}\sigma^{el} \tag{2}$$

Furthermore, the plastic strain rate $\dot{\varepsilon}^{pl}$ is governed by the associated flow rule, given by:

$$\dot{\varepsilon}^{pl} = \dot{\lambda}\frac{\partial f}{\partial \sigma}, \dot{\lambda} \geq 0 \text{ if } f = 0 \text{ and } \dot{f} = 0, \text{otherwise } \dot{\lambda} = 0 \tag{3}$$

where $f(\sigma)$ is the yield function, which defines a convex surface in stress space when $f(\sigma) = 0$.

During the simulations, the equivalent plastic strain was calculated and used to evaluate the plastic performance of the structure, which is a scalar quantity that represents the accumulated plastic deformation in the material. It can be expressed with the following formula:

$$\bar{\varepsilon}^{pl} = \int_0^t \sqrt{\frac{2}{3}\dot{\varepsilon}_{ij}^{pl}\dot{\varepsilon}_{ij}^{pl}}\,dt \tag{4}$$

where $\dot{\varepsilon}_{ij}^{pl}$ is the plastic strain rate tensor, and $t$ denotes time.

## 3 FINITE ELEMENT MODEL

This section provides a detailed overview of the constructed FE model, which was used to demonstrate the potential and effectiveness of the proposed optimization framework. To ensure reliable results, the model was validated under monotonic loading against the experimental tests documented in the seminal work of Bursi and Jaspart [15]. Subsequently, a dynamic load was applied to this initial configuration, and the equivalent plastic strain values were calculated. The geometric properties of the developed model are illustrated in Figure 2.

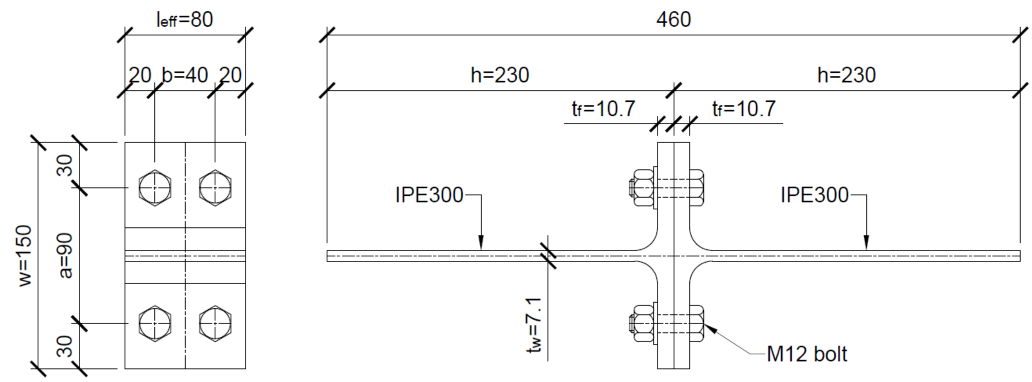


Figure 2: The geometric properties of the considered configuration.

The FE model was constructed from 8-node linear brick elements with reduced integration (C3D8R). A general mesh size of 5mm was employed for IPE300 T-stub section, and 2mm for the bolts, as presented in Figure 3, which additionally contains the boundary and load conditions.

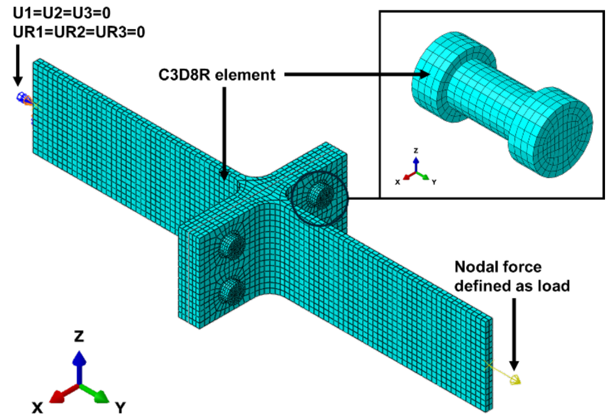


Figure 3: The developed FE model of the considered configuration.

During the simulation, an elastic-plastic material model of steel with isotropic hardening was utilized. The material properties were adopted from [15], and the key characteristics are summarized in Table 1, categorized separately for the flange plate, web plate, and bolts. This approach enables accurate analysis and precise calculation of plastic strain, reflecting real-life conditions.

| Part | Modulus of elasticity $(N/mm^2)$ | Yield stress $(N/mm^2)$ | Ultimate tensile stress $(N/mm^2)$ |
|---|---|---|---|
| Section's flange | 240,782 | 431 | 787 |
| Section's web | 217,130 | 469 | 787 |
| Bolt | 160,612 | 893 | 1025 |

Table 1: The main material properties of the analyzed configuration.

To accurately reflect the real-life structural behavior of bolted connections, simulating friction interactions between different components of the assembly is essential. Therefore, the FE model was constructed using the "surface-to-surface" contact method, employing the penalty formulation for tangential behavior with a friction coefficient of 0.30 and "hard" contact for normal behavior.

For enhanced accuracy, a geometrically nonlinear analysis was conducted to account for the effects of large deformations. The results of the simulation under monotonic loading, performed on the proposed model, closely correspond to the experimental tests presented in [15], as illustrated in Figure 4. A detailed comparison indicates that the variation in the initial stiffness value was 1.23%, while the difference in the ultimate force was only 0.23%.

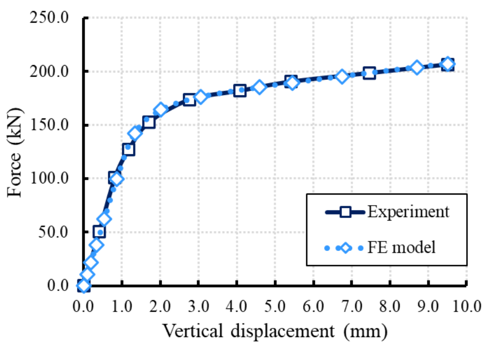


Figure 4. The comparison between the results of the constructed FE model and the experimental test.

In a later phase, dynamic loading was applied to the configuration, with its characteristics and the corresponding force-displacement relationship illustrated in Figure 5. The results indicated that, with the previously presented bolt layout, the maximum equivalent plastic strain reached 4.20% in the T-stub section and 6.01% in the bolts.

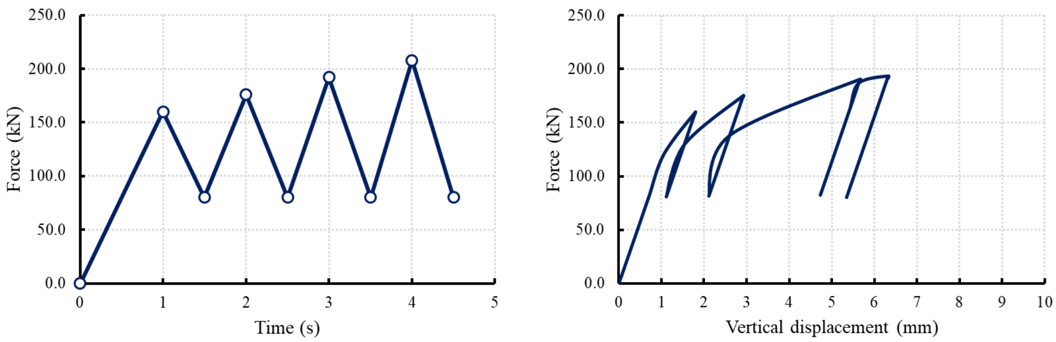


Figure 5: The applied cyclic force over time and the corresponding force-displacement relationship.

## 4 OPTIMIZATION FRAMEWORK

This section outlines the key elements of the developed framework, detailing the problem formulation of the optimization process and its implementation. Furthermore, the results are analyzed and discussed.

### 4.1 Problem formulation and implementation

In this part, the developed optimization framework is presented, emphasizing the key elements. Its primary objective is to minimize plastic deformation of the given configuration by determining the optimal bolt positions. Consequently, the optimization problem can be formulated as follows:

$$Min: \quad \bar{\varepsilon}^{pl} = \int_0^t \sqrt{\frac{2}{3}\dot{\varepsilon}_{ij}^{pl}\dot{\varepsilon}_{ij}^{pl}}\,dt \tag{5}$$

$$Subject\ to: \quad \bar{\varepsilon}^{pl} \leq \bar{\varepsilon}_{max}^{pl} \tag{6}$$

$$\mathrm{e} \geq 1.2d \tag{7}$$

$$p \geq 2.4d \tag{8}$$

In this context, Eq. (5) represents the objective function, which aims to minimize the equivalent plastic strain during the cyclic loading process. Additionally, Eq. (6) is introduced to control plastic deformations, where $\bar{\varepsilon}_{max}^{pl}$ denotes the allowable plastic strain, set to 5.00% in accordance with the Eurocode recommendation [34]. Furthermore, Eqs. (7) and (8) define the design criteria based on EN 1993-1-8 [8], where $e$ denotes the edge distance from the center of the bolt hole, and $p$ represents the spacing between bolt centers. Based on these constraints, the search space for bolt positions was set to vary within specified limits: in the transverse direction ($a$), it ranged from $57mm$ to $120mm$ in $1.00mm$ discrete steps, while in the longitudinal direction ($b$), it varied from $26mm$ to $50mm$ in $0.75mm$ discrete steps.

To accomplish the main objective of the research, Eqs. (5)-(8) were integrated into a developed code implemented in the PYTHON programming language and linked to ABAQUS software [25]. This script incorporates the GA, including all its key elements, allowing the automatic determination of the optimal bolt layout. For further clarification, during the optimization process, the initial population is created based on the design domain in the form of standard bit-string chromosomes. Subsequently, the FE models are constructed according to the encoded chromosomes, and simulations are conducted. Once the analysis is completed, the developed code calculates the fitness, which corresponds to the equivalent plastic strain, based on the results.

Genetic operators are then applied to generate the offspring population, including tournament selection, uniform crossover, and mutation. Additionally, an elitist operator is incorporated to automatically transfer the two best individuals to the next generation. This iterative process continues until the final generation is reached, as illustrated in Figure 6. Furthermore, the key properties of the GA are summarized in Table 2.

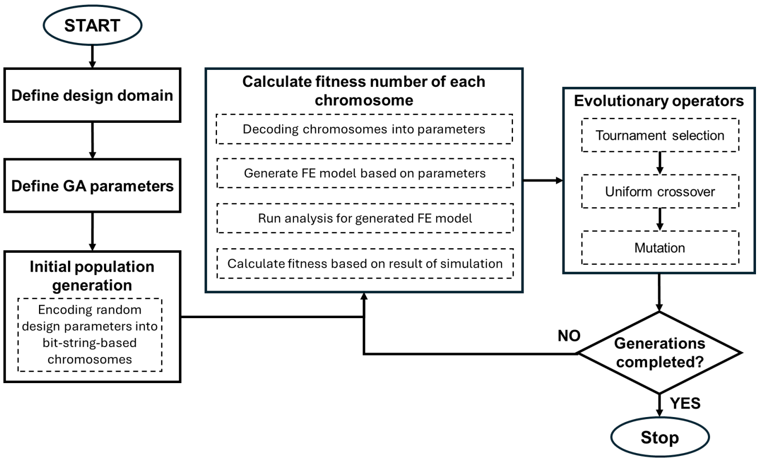


Figure 6: The operation of the developed optimization framework

| Parameter | Value |
|---|---|
| Number of generations | 10 |
| Population size | 20 |
| Crossover probability | 0.7 |
| Mutation probability | $0.1 - 0.9$ |
| Tournament size | 2 |
| Elitism size | 2 |

Table 2: The key properties of the GA.

## 4.2 Results and discussion

As previously mentioned, to demonstrate the efficiency of the proposed framework, the optimal layout of the presented FE model was determined using the developed code. Accordingly, Figure 7 illustrates the evolution history of the minimum and average strain values with respect to the current generation, where it can be observed that after the fourth generation, values starting to get stabilized.

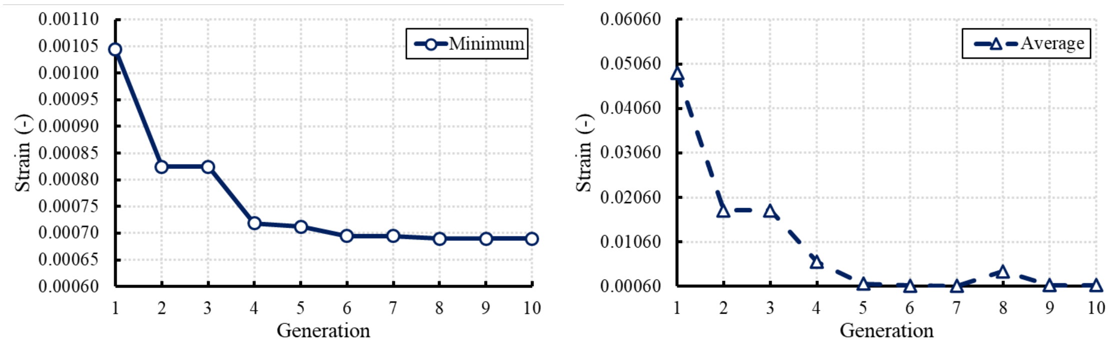


Figure 7: Evolution history of the minimum and average strain values.

Remarkably, a significant reduction in plastic deformation was achieved in both the T-section and bolts solely by optimizing the bolt positions, as shown in Table 3 and further illustrated in Figure 8. It can be observed that plastic strain was significantly diminished by approximately 95.84% compared to the initial configuration, calculated as the difference between the optimal and initial solutions, expressed as a percentage of the initial value. This suggests that under dynamic effects, such as those caused by earthquakes, a notable improvement in seismic resilience can be attained, thereby minimizing damage and enhancing safety. Moreover, this contributes to a more sustainable design by mitigating material degradation without requiring additional resources.

| Configuration | Distance between bolts | | Maximum plastic strain | |
|---|---|---|---|---|
| | Transverse direction $a$ | Longitudinal direction $b$ | T sections | Bolts |
| Initial | $90.0mm$ | $40.0mm$ | 4.20% | 6.01% |
| Optimal | $59.0mm$ | $40.3mm$ | 0.06% | 0.25% |

Table 3: Comparison between the initial and optimal configuration

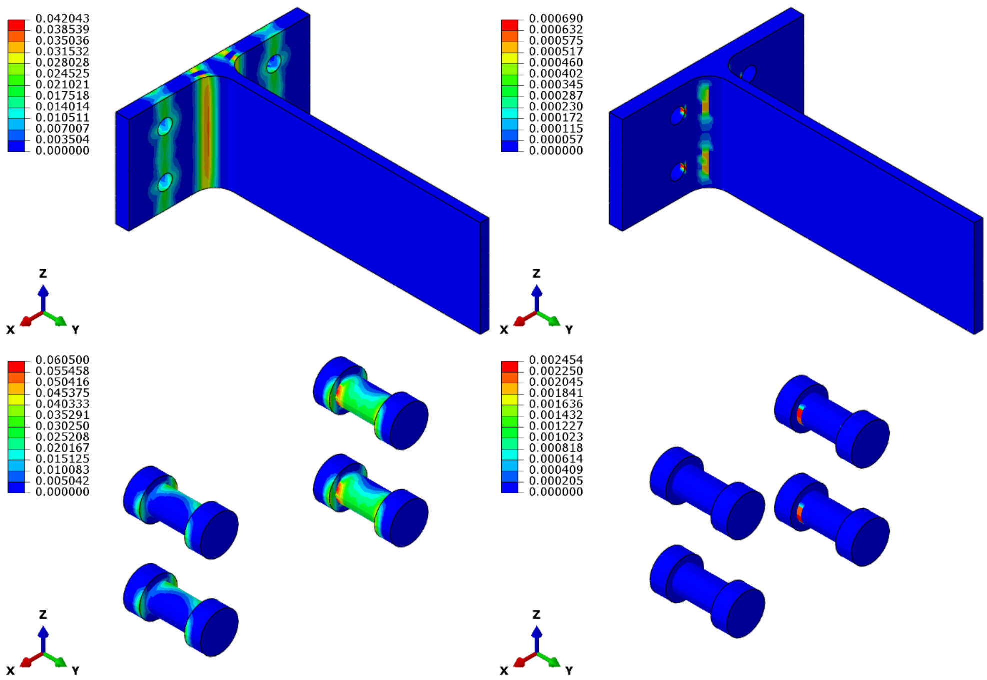

Figure 8: Equivalent plastic strain distribution in the T-section and bolts under cyclic loading for the initial and optimal configurations.

## 5 CONCLUSIONS

In this paper, an optimization framework was introduced to minimize plastic deformations in T-stub connections under dynamic loading conditions by optimally determining bolt positions. This approach enhances seismic resilience and improves sustainability, as no additional material is required for the configuration, yet significant damage reduction can be attained.

To accomplish this, a nonlinear finite element code was developed, incorporating elasto-plastic material behavior, large deformations, and contact properties. The implementation was carried out using the PYTHON programming language and ABAQUS software. The proposed framework was tested on a selected bolted T-stub configuration and validated against experimental results. To determine the optimal bolt positions, a genetic algorithm was integrated into the code, enabling automated design. Additionally, constraints were incorporated into the optimization process, formulated based on Eurocode criteria, to further enhance the safety of the configuration.

The results obtained through the proposed framework indicate that a substantial reduction in plastic deformation can be realized solely by optimizing the bolt layout. In the developed FE model, plastic strain was reduced by 95.84%. This remarkable outcome highlights the potential and effectiveness of the developed methodology, which enhances sustainability by improving safety without requiring additional material.

## REFERENCES


[1] A. W. Lacey, W. Chen, H. Hao, and K. Bi, Review of bolted inter-module connections in modular steel buildings, in *Journal of Building Engineering*, **23**, 2019.

[2] B. Yang and K. H. Tan, Experimental tests of different types of bolted steel beam-column joints under a central-column-removal scenario, *Engineering Structures*, **54**, 112–130, 2013.

[3] X. Wang, P. Wang, and W. Chen, Test on progressive collapse of steel moment-resisting frame with upper-and-lower flange angle steel connection, *Structures*, **68**, 2024.

[4] J. Becque, P. Desnerck, R. Crawforth, and J. Guo, Experimental investigation and analytical prediction of the rotational stiffness of apex connections in cold-formed steel portal frames, *Thin-Walled Structures*, **209**, 2025.

[5] Z. Tang, Z. Li, T. Wang, D. Lu, and Y. Tan, PDEM-based multi-component and global reliability evaluation framework for steel tubular transmission towers with semi-rigid connections, *Engineering Structures*, **295**, 2023.

[6] J. Becque, P. Desnerck, R. Crawforth, and J. Guo, Experimental investigation and analytical prediction of the rotational stiffness of apex connections in cold-formed steel portal frames, *Thin-Walled Structures*, **209**, 2025.

[7] Y. Zhang, J. Zhan, Y. Liao, W. Ding, S. Tan, and Y. Liu, Experimental and numerical studies on hybrid bolted connection of steel box girders: Bending mechanism, *Engineering Structures*, **321**, 2024.

[8] European Committee for Standardisation, *EN 1993-1-8: Eurocode 3: Design of steel structures - Part 1-8: Design of joints*, 2005.

[9] M. Byfield, W. Mudalige, C. Morison, and E. Stoddart, A review of progressive collapse research and regulations, *Proceedings of the Institution of Civil Engineers - Structures and Buildings*, **167**, 447–456, 2014.

[10] ARUP, *Review of international research on structural robustness and disproportionate collapse*, London: Department for Communities and Local Government, 2011.

[11] P. Grubits, T. Balogh, and M. Movahedi Rad, Optimization of Bolted Steel T-Stub Connection Based on Nonlinear Finite Element Analysis Using Genetic Algorithm, *Infrastructures*, **10**, 2025.

[12] M. M. Rad, F. Papp, S. K. Ibrahim, J. Szép, D. Gosztola, and D. Harrach, Elasto-plastic analysis and optimal design of composite integral abutment bridge extended with limited residual plastic deformation, *Scientific Reports*, **13**, 2023.

[13] P. Grubits, R. Cucuzza, M. Habashneh, M. Domaneschi, P. Aela, and M. Movahedi Rad, Structural topology optimization for plastic-limit behavior of I-beams, considering various beam-column connections, *Mechanics Based Design of Structures and Machines*, 2024.

[14] P. Grubits, R. Cucuzza, D. Gosztola, M. Domaneschi, J. Szép, and M. Movahedi Rad, Numerical Modeling of Multi-Pass Arc Welding Processes: Integration with Experimental Validation for Distortion analysis and Characterization, in *Advances in Transdisciplinary Engineering*, **59**, IOS Press BV, 2024.

[15] O. S. Bursi and J. P. Jaspart, Benchmarks for Finite Element Modelling of Bolted Steel Connections, *J. Construct. Steel Res.*, **43**, 17–42, 1997.

[16] Z. Al-Khatab and A. Bouchaïr, Analysis of a bolted T-stub strengthened by backing-plates with regard to Eurocode 3, *Journal of Constructional Steel Research*, **63**, 1603–1615, 2007.

[17] M. A. Bravo and R. A. Herrera, Performance under cyclic load of built-up T-stubs for Double T moment connections, *Journal of Constructional Steel Research*, **103**, 117–130, 2014.

[18] J. Ribeiro, A. Santiago, C. Rigueiro, P. Barata, and M. Veljkovic, Numerical assessment of T-stub component subjected to impact loading, *Engineering Structures*, **106**, 450–460, 2016.

[19] H. R. Sebbagh, D. E. D. Kerdal, A. Abidelah, and A. Bouchaïr, T-stubs with two and four bolts under monotonic and cyclic loading, *Journal of Constructional Steel Research*, **178**, 2021.

[20] X. Huang, R. Li, X. Zhang, J. Ge, and J. Zhao, Ultra low cycle fatigue behavior of Q690 high-strength steel welded T-stub joints: Experiments and fracture prediction analysis, *Thin-Walled Structures*, **191**, 2023.

[21] W. Wang, H. Fang, and Z. Wang, Comprehensive studies on the behaviors of high strength steel T-stubs with thin-walled flange at elevated temperatures, *Thin-Walled Structures*, **190**, 2023.

[22] A. Kaveh and P. Zakian, Optimal design of steel frames under seismic loading using two meta-heuristic algorithms, *Journal of Constructional Steel Research*, **82**, 111–130, 2013.

[23] A. Kaveh, M. H. Ghafari, and Y. Gholipour, Optimum seismic design of steel frames considering the connection types, *Journal of Constructional Steel Research*, **130**, 79–87, 2017.

[24] J. Liu, C. Qiu, X. Du, and H. Liu, Seismic performance evaluation of a novel resilient steel frame with self-centering rocking columns and replaceable energy-dissipating connections for low-rise structures, *Engineering Structures*, **303**, 2024.

[25] Michael Smith, ABAQUS/Standard User's Manual, Version 6.9, Dassault Systèmes Simulia Corp, United States, 2009.

[26] J. H. Holland, Genetic Algorithms and Adaptation, in *Adaptive Control of Ill-Defined Systems*, Springer US, Boston, MA, 1984.

[27] O. Kramer, *Genetic Algorithm Essentials*, Springer International Publishing, 2017.

[28] T. Balogh and L. G. Vigh, Optimal fire design of steel tapered portal frames, *Periodica Polytechnica Civil Engineering*, **61**, 824–842, 2017.

[29] F. Di Trapani, A. P. Sberna, and G. C. Marano, A new genetic algorithm-based framework for optimized design of steel-jacketing retrofitting in shear-critical and ductility-critical RC frame structures, *Engineering Structures*, **243**, 2021.

[30] G. Li, Z. Li, Q. Zeng, and X. Guo, Shape optimization of cast steel tubular joints based on subdivision surface and genetic algorithm, *Thin-Walled Structures*, **204**, 2024.

[31] M. O. Okwu and L. K. Tartibu, *Metaheuristic Optimization: Nature-Inspired Algorithms Swarm and Computational Intelligence, Theory and Applications*, Springer, 2021.

[32] J. Yang and C. K. Soh, Structural Optimization by Genetic Algorithms with Tournament Selection, *Journal of Computing in Civil Engineering*, **11**, 195–200, 1997.

[33] D. E. Goldberg and K. Deb, A Comparative Analysis of Selection Schemes Used in Genetic Algorithms, *Foundations of Genetic Algorithms, **1***, 69-93, 1991.

[34] European Committee for Standardisation, *EN 1993-1-5: Eurocode 3: Design of steel structures - Part 1-5: General rules - Plated structural elements*, 2006.